SINTEF

OC2019 A-111 - Open

Report

Spreading and potential effects of marine fuel oil spills in the Arctic

ARCTICFUELS

Author(s)
Bjørn Henrik Hansen
Julia Farkas, Bjarne Kvæstad, Per S. Daling, Liv-Guri Faksness & Jørgen Skancke

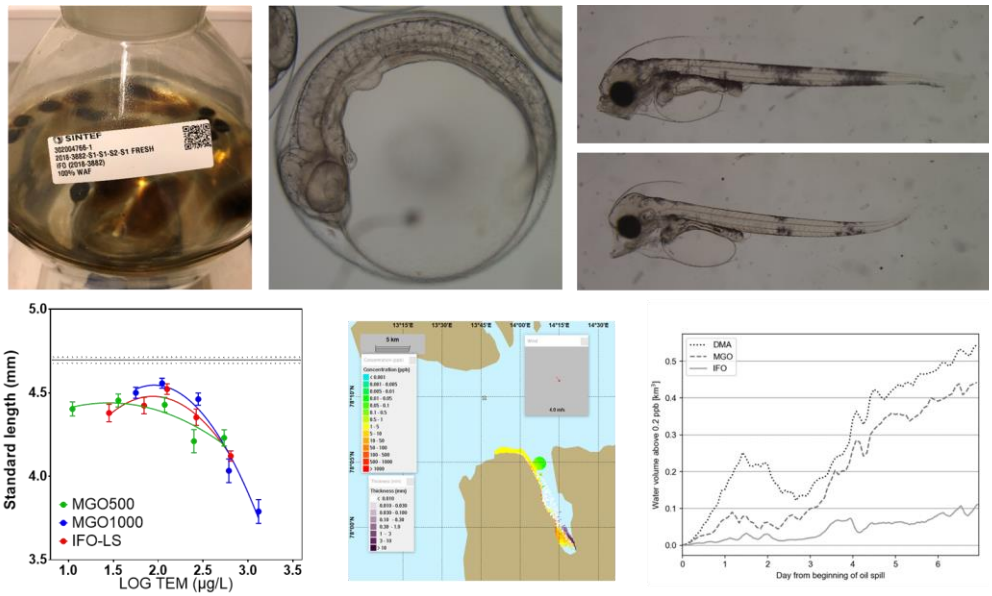

SINTEF Ocean AS

2019-09-04

SINTEF

Report

Spreading and potential effects of marine fuel oil spills in the Arctic

ARCTICFUELS

REPORT NO.	PROJECT NO.	VERSION	DATE
OC2019 A-111	302004766	1.0	2019-09-09

KEYWORDS:
Arctic
Fuel
Marine
Ecotoxicity
Fish
PAH
Oil spill
Modelling

AUTHOR(S)
Bjørn Henrik Hansen
Julia Farkas, Bjarne Kvæstad, Per S. Daling, Liv-Guri Faksness & Jørgen Skancke

CLIENT(S)
Svalbard Miljøvernfond

CLIENT'S REF.	NUMBER OF PAGES/APPENDICES:
Sysselmannen Svalbard v/Heidi Eriksen	23

CLASSIFICATION	CLASSIFICATION THIS PAGE	ISBN
Open	Open	978-82-7174-367-3

ABSTRACT
In the ARCTICFUELS project we studied the effects of dissolved fractions of three fuel oils (MGO500, MGO1000 and IFO-LS) on developing cod embryo and larvae. Of the three fuel oils tested, the MGO1000 displayed the highest toxicity when comparing toxicity based on dilution (% of initial water accommodated fraction, WAF), however, when related to mass in terms of total extractable material (TEM), the concentration-dependent responses followed similar trends for the three oils. Even after diluting WAFs to 6%, we were unable to reach an exposure level that did not cause any toxicity, so establishing no effect concentration (NEC) thresholds was not possible. OSCAR-based oil spill simulations in Isfjorden (Svalbard) were performed for all three fuel oils. These simulations indicated that the potential for toxicity to early life stages of fish were significantly higher for MGO1000 compared to MGO500 and IFO-LS. The composition of the MGO1000 facilitates dissolution as it contains high content of dissolvable components, including PAHs, which are expected to cause developmental effects on fish early life stages.

PREPARED BY	CHECKED BY	APPROVED BY
Bjørn Henrik Hansen	Trond Nordtug	Mimmi Throne-Holst

Document History

VERSION	DATE	VERSION DESCRIPTION
1.0.	2019-09-04	Draft version sent to and approved by clients

SINTEF

Table of Contents

Abstracts

Norsk sammendrag

I ARCTICFUELS-prosjektet studerte vi effekten av vann-løste komponenter av tre marine drivstoff (MGO500, MGO1000 og IFO-LS) på utvikling av torskembryo og -larver. Av de tre testede drivstoffene viste MGO1000 den høyeste giftigheten ved sammenligning av toksisitet basert på % fortynning av den innledende vann-løste fraksjonen. Relatert til masse løste oljekomponenter (totalt ekstraherbart materiale), fulgte de konsentrasjonsavhengige responsene lignende trender for de tre oljene. Selv i den mest fortynnede løsningen (6%), klarte vi ikke å nå et eksponeringsnivå som ikke forårsaket noen giftighet. Derfor var det ikke mulig å etablere nulleffekt-konsentrasjonsgrenser (NEC). Oljeutslippssimuleringer med bruk av OSCAR-modellen ble gjennomført for alle tre drivstoffene i Isfjorden (Svalbard). Disse indikerte at potensialet for å forårsake skader på tidlige livsfaser for fisk var betydelig høyere for MGO1000 sammenlignet med MGO500 og IFO-LS. Dette er forårsaket av at MGO1000 inneholder et høyt innhold av løselige komponenter, inkludert polysykliske aromatiske hydrokarboner (PAH), som forventes å gi utviklingseffekter på fiskens tidlige livsfaser.

English Abstract

In the ARCTICFUELS project we studied the effects of dissolved fractions of three fuel oils (MGO500, MGO1000 and IFO-LS) on developing cod embryo and larvae. Of the three fuel oils tested, the MGO1000 displayed the highest toxicity when comparing toxicity based on dilution (% of initial water accommodated fraction, WAF), however, when related to mass in terms of total extractable material (TEM), the concentration-dependent responses followed similar trends for the three oils. Even after diluting WAFs to 6%, we were unable to reach an exposure level that did not cause any toxicity, so establishing no effect concentration (NEC) thresholds was not possible. OSCAR-based oil spill simulations in Isfjorden (Svalbard) were performed for all three fuel oils. These simulations indicated that the potential for toxicity to early life stages of fish were significantly higher for MGO1000 compared to MGO500 and IFO-LS. The composition of the MGO1000 facilitates dissolution as it contains high content of dissolvable components, including polycyclic aromatic hydrocarbons (PAHs), which are expected to cause developmental effects on fish early life stages.

1 Background and Relevance

The new bans against carrying heavy fuel oil (HFO) on vessels in certain areas around Svalbard, has been implemented based on expected environmental gain in the event of accidental discharges. Low viscosity and less persistent oils such as light distillate marine fuels (e.g marine gas oils; MGO) will have a reduced "lifetime" on the sea surface due to higher degree of natural dispersion into the water column leading to increased biodegradability. Therefore, in nature reserves and national parks on Svalbard, it is now only allowed to use light DMA quality fuel oils (ISO 8217: 2017 standard). On the other hand, it is permitted to use other fuel qualities, such as wide range gas oil, WRG and heavy fuel oils, outside these areas.

The establishment of SECA (Sulphur Emission Control Area), set out in Annex VI of the MARPOL Convention, demanded < 0.1% sulphur in marine fuel oils by 2015, and by 2020 a demand of < 0.5% sulphur will be in place in the global requirements to reduce emissions of sulphur oxide (SOx) and nitrogen oxide (NOx) from vessels. These regulations have led to new fuel products coming on the market, often called hybrid oils or low sulphur fuel oils (LSFO). This new generation of LSFO oils are divided into two categories according to the Sulphur limits: Ultra Low Sulphur Fuel Oil (ULSFO: S < 0.1%) and Very Low Sulphur Fuel Oils (VLSFO: < 0.5 %S). Hybrid oil properties vary from product to product, and they are designed to have low sulphur content while not requiring rebuilding of vessel engines. However, they are not defined as DMA quality, and can only be used outside nature reserves on Svalbard. In the recent years, there have been an increase in carrying LSFO oils also in Arctic areas (DNVGL, 2019), and this will increase further with the new demands from 2020.

Although the environmental benefits in the form of lower emissions to air are taken care of through Annex VI, and a reduced lifetime of oil spills on the sea is taken care of by the heavy oil ban, there is relatively little knowledge about the other possible environmental benefit / drawbacks if an acute accidental spill would occur with the new LSFO-fuels and the different DMA distillate properties used today, compared to the earlier "traditional" HFOs.

SINTEF has earlier carried out both scenario-based modelling studies (Kystverket, 2014), and toxicity studies of water accommodated fractions (WAF) from six different marine fuel oils on marine algae (*Skeletonema costatum*) and copepods (*Calanus finmarchicus*) showed that the most toxic tested product was a DMA-quality marine diesel from the Shell-refinery in Rotterdam (Hellstrøm, 2017). These studies should be supplemented with toxicity tests also at a higher trophic level. Early life stages of fish have been shown to be particularly sensitive to oil exposure (Hansen et al., 2018a; Sørhus et al., 2015) and it is necessary to establish threshold values also for such organisms. Threshold values for toxicity for different organisms are essential inputs for predicting potential effects associated with accidental releases, as well as evaluating response actions that must be initiated after accidental spills.

2 Aim and Objectives of ARCTICFUELS

The main aim of the project was to evaluate the potential for different marine fuels to cause harmful effects on sensitive life stages of fish in marine Arctic waters.

The results have high relevance for authorities with administrative responsibility related to maritime transport and the environment in Norway in general, and around Svalbard in particular. Environmental protection authorities that are prepared to respond to acute pollution in protected areas will be able to use the results of this project as input to emergency preparedness for acute discharges of marine fuel in vulnerable areas around Svalbard.

The ARCTICFUELS project had the following objectives:

1. **Perform toxicity testing of different fuel oils using highly sensitive early life stages of cold-water fish**
2. **Perform oil spill simulations to estimate spreading of fuel oil in the water column and resulting concentrations during acute spills from different fuel oils**

The project compared time-integrated water volumes containing fuel oil concentrations expected to cause effects on fish early life stages between different fuel oils, and thus generated a ranking of the selected fuel oils in terms of risk to cause effects on these sensitive organisms.

3 Materials and Methods

3.1 Choice of marine fuels

Three marine fuel oils were chosen for the present study; a marine diesel from the Rotterdam refinery, a marine gas oil from Esso Slagen and a heavy fuel oil (IFO 180) supplied by Kystverket. The marine diesel and gas oils are both DMA quality, and but referred to as MGO1000 and MGO500 in the report, whereas the heavy fuel oil is referred to as IFO-LS. The fuel oils were used as fresh products, and not weathered in any way.

Table 3.1: Sample description, SINTEF ID, labels and properties of the marine fuel oils used in this study.

Fuel type	**Rotterdam diesel**	**Marine gas oil 500 ppm S**	**IFO 180**
Notation	MGO1000	MGO500	IFO-LS
SINTEF ID	2016-0232	2014-0551	2018-3882 (2014 batch)
Sulphur content	0,09 %	0,05 %	<1%
	Marine gas oil (dyed) from Rotterdam, DMA-quality	Marine gas oil with max. 500 ppm sulphur, DMA-quality	
Kilde	Shell	Esso Slagen	Kystverket (Shell refinery 2014)
Density (g/ml)	0,885	0,852	0,961
Flash point (°C)	62,5	82,5	88,5
Pour point (°C)	<-36	<-36	18
Asphaltenes (vekt%)	0,02	0,02	5-6%
Wax (vekt%)	3,1	0,81	4-5%

3.2 Preparation of exposure solutions

Preparation of low energy WAF (LE-WAF) was performed under controlled conditions following the guidelines established by the Chemical Response to Oil Spills: Ecological Research Forum (CROSERF). These guidelines were developed to standardize WAF preparation, laboratory exposures to aquatic organisms, and analytical chemistry measurements used to determine the acute toxicity of the water soluble components in the oil (Aurand and Coelho, 1996). LE-WAF can be defined as a water solution of dissolved oil components prepared in closed vessels, as shown in the picture in Figure 3.1, with calm mixing of oil and water without the formation of any vortex. LE-WAFs were chosen in order to avoid generation of oil droplets as these may stick to eggs and thereby contribute to an additional exposure to passive diffusion (Hansen et al., 2018b).

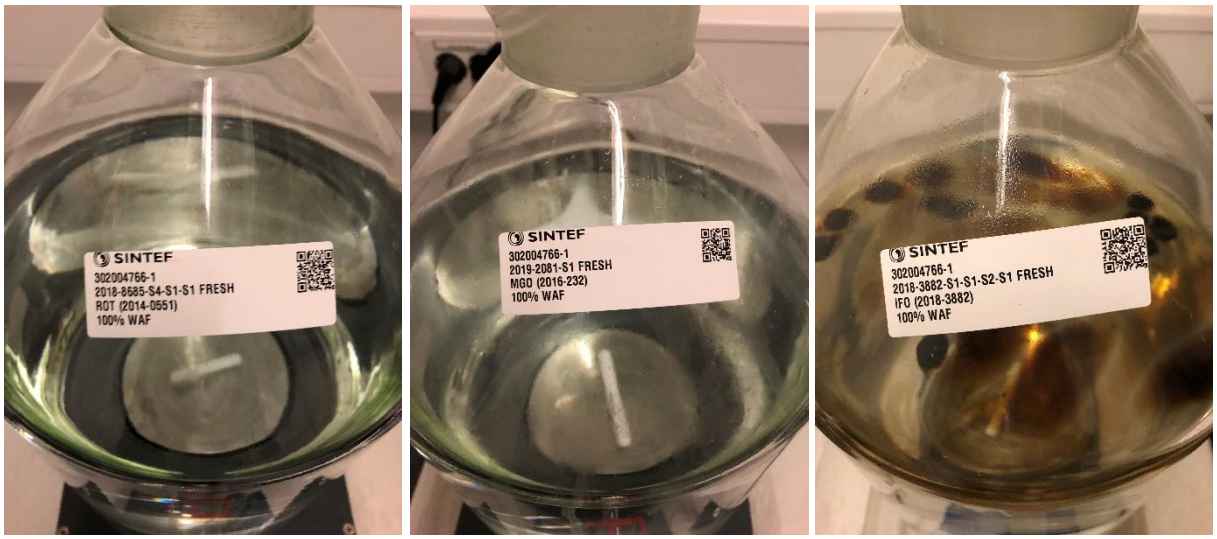

Figure 3.1: LE-WAF systems of fresh fuel oil products with oil to water ratios of 1 to 10 000 for MGO1000 (left), MGO500 (middle) and IFO-LS (right).

3.3 Water sampling and chemical analyses

Surrogate internal standards (SIS, o-terphenyl, naphthalene-d_8, phenanthrene-d_{10}, chrysene-d_{12}, phenol-d_6, 4-methylphenol-d_8) were added to the water samples prior to processing, and recovery internal standards (RIS, 5α-androstane, fluorene-d_{10}, and acenaphthene-d_{10}) were added prior to analysis on GC/FID (gas chromatography/flame ionization detection) and GC/MS (gas chromatography/mass spectrometry). For analyses of semi-volatile organic compounds (SVOC) and total extractable material (TEM), the water samples were serially extracted with dichloromethane (DCM), thereby following a modification of EPA method 3510C (USEPA, 1996). The combined extracts were dried with sodium sulphate and concentrated to approximately 1 mL using a Zymark Turbovap® 500 Concentrator. The final extract was used for analyses.

The samples were analyzed for SVOC (decalins, PAHs and phenols) using GC/MS, for TEM using GC/FID, and for volatile organic compounds (VOC, C5-C9), including BTEX (benzene, toluene, ethylbenzene, and xylenes), by use of P&T GC/MS (Purge and Trap Gas Chromatography Mass Spectrometry). This target list includes the recommended analytes given by Singer et al. (2000), and is a typical standard list for the target compounds used during post-oil spill damage assessments.

The GC/FID analyses were performed according to a modification of EPA Method 8015D (US-EPA, 2013). TEM (resolved plus unresolved TEM) was quantified by the method of internal standards using the baseline corrected total area of the chromatogram and the average response factor for the individual C_{10} to C_{36} n-alkanes. The semi-volatiles were quantified by modifications of EPA Method 8270D (USEPA, 2007). The mass spectrometer was operated in the selective ion monitoring mode to achieve optimum sensitivity and specificity. The quantification of target compounds was performed by the method of internal standards, using average response factors (RF) for the parent compounds. The PAH and phenol alkyl homologues were quantified using the straight baseline integration of each level of alkylation and the RF for the respective parent PAH compound. The response factors were generated for all targets and surrogates versus fluorened10. A total of 35 target volatile analytes in the C_5 to C_{10} range were determined by P&T GC/MS using a modification of EPA method 8260C (US-EPA, 2006). The samples were spiked with SIS (toluene-d_8 and ethylbenzene-d_8) and RIS (chlorobenzene-d_5). The quantification of individual compounds was performed by

using the RFs of the individual compounds relative to the internal standards. All standards and samples were analysed in a full scan mode.

3.4 Exposure of fish eggs

Eggs and milt from adult Atlantic cod (*Gadus morhua*) eggs were collected through strip-spawning of adult fish from brood stocks kept in 7000 L tanks at Austevoll Research Station at the Institute of Marine Research (IMR). Fertilized eggs (300 ml) were transferred to sea water in closed bottles which were insulated with bubble wrap, placed on ice in a styrofoam container and sent to SINTEF Sealab in Trondheim using airfreight. At arrival, less than 12 hours after fertilization, eggs were transferred to 50 L tanks with flow-through of filtered (1 µm) seawater (6 ± 1°C) delivering one volume exchange of seawater per day. Natural sea water, collected from a depth of 80 m (below thermocline) in a nonpolluted Norwegian fjord (Trondheimsfjord; 63°26' N, 10°23' E), was supplied by a pipeline system from the source to our laboratories (salinity of 34 ‰, pH 7.6). Gentle air bubbling kept embryos moving continuously in the tanks. Dead and unfertilized eggs were removed from the tank daily. The embryos were acclimated for 4 days until being transferred to glass jars for exposure.

The LE-WAFs generated from the three oils were diluted with filtered sea water at nominal concentrations of 6, 12, 25, 50 and 100 (undiluted) % solutions. These solutions were transferred to glass jars (100 ml) and used to expose fish eggs (approx. 100 eggs in each jar) for 4 days (4-8 dpf). After 2 days exposure an additional 100 ml of fresh exposure solution was supplied to each jar to compensate for the initial loss of oil components. All treatments were run with four replicates (N=4). After 4 days exposure, dead eggs were counted and removed, and the surviving eggs were transferred to clean glass jars containing clean sea water (100 mL) and maintained at 6 ± 1°C until 3 days post hatch (3 dph). Survival and hatching were monitored throughout the recovery period. Images and videos of 6-12 larvae (3 dph) from each replicate were taken through a microscope (Eclipse 80i, Nikon Inc., Japan) equipped with Nikon PlanApo objectives (2x for whole larvae images and 10x for close-up larvae images and videos), a 0.5x videoadaptor and a CMOS camera (MC170HD, Leica Microsystems, Germany).

3.5 Morphometry

Larvae images were used for biometric analyses using automated analyses and blinded deformation ranking analysis adopted from Sørhus et al (2015) and Hansen et al (2018a). All larvae were analyzed for standard length, body area, yolk sac area, myotome height, eye area and eye-to-forehead distance. Representative images of larvae with highlighted traces of distances/areas are given in Figure 3.2.

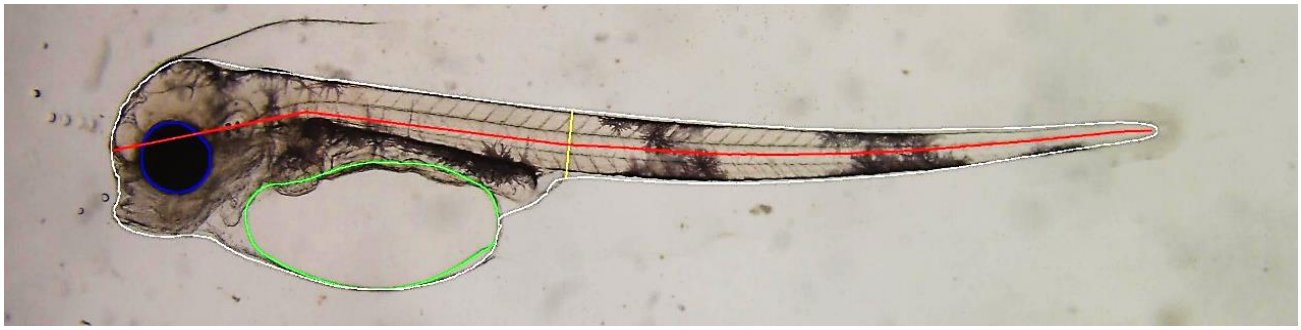

Figure 3.2: Example of a cod larvae with highlighted automated measurements. White, green and blue lines display the area surrounding the body, yolk sac and eye, respectively. The red line displays the standard length and yellow line represents the myotome height.

Morphological abnormalities (jaw deformations, craniofacial deformations, pericardial edema and spine deformations) were determined for larvae (3 dph) according to a severity degree scale (1-3 where 1 is normal, 2 is moderate deformation and 3 is severe deformation) similar to previous studies (Hansen et al., 2018a; Hansen et al., 2019; Sørensen et al., 2019; Sørhus et al., 2015). Examples of control and deformed larvae (3 dph) are given in Figure 3.3.

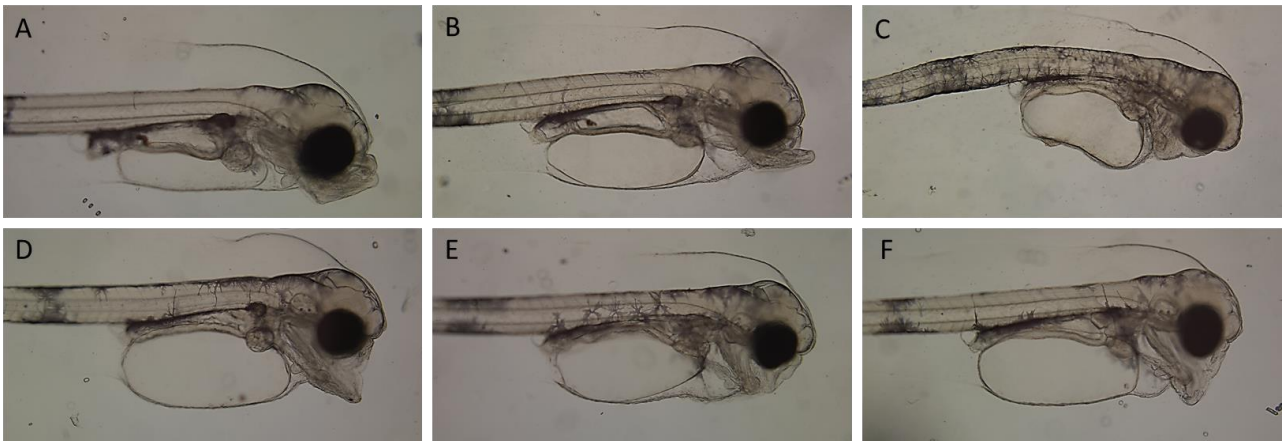

Figure 3.3: Examples of a cod larvae with deformations. A: Normal cod larvae. B-F: cod larvae with various craniofacial/jaw deformations and pericardial edema (B, E and F).

3.6 Cardiac activity

Microscopy videos were used as a basis for monitoring heart rate (HR) in individual larvae using automated video analyses. Briefly, this method identifies the heart tissue region in the video through pixel intensity difference between frames. Then, the time sequence of mean value of the intensity in that region is extracted. This signal tends to oscillate in concert with heart contraction and expansion. After normalization and smoothing the signal, the number of peaks is counted, which is interpreted as the number of heart beats, providing an estimate of the heart rate. The method also performs an analysis of the video and signal quality, which is used to indicate potential outliers (e.g. non-beating hearts, strong larval motion) (Nepstad et al., 2017).

3.7 Data treatment

Statistical analyses were conducted using GraphPad Prism statistic software, V6.00 (GraphPad Software, Inc., CA, USA). Treatments were compared using one-way ANOVA followed by Tukey's multiple comparisons test. The significance level was set at $p < 0.05$ unless otherwise stated. Nonlinear curve fit (third-order polynomial) was used in figures displaying effects as a function of exposure.

3.8 Oil spill scenario modelling using the OSCAR model

In the event of an accident, large amounts of fuel oil may leak from vessels after collision or grounding in relatively short time. After leaking to the ocean, the oil will be subject to weathering and dispersion at sea.

The concentration of dissolved oil components in the water column, and therefore the potential exposure to pelagic organisms, will depend on the ambient conditions in terms of wind, waves, and currents. These determine the degree of evaporation, vertical mixing, horizontal mixing, and dissolution from surface slicks and entrained oil droplets. In addition, geographic constrains near shore may reduce mixing and cause enhanced concentrations compared to the open sea. Further, the extent to which the different processes dominate in an oil spill is influenced by the composition and physiochemical properties of the spilled oil. In this regard, the MGO500 and MGO1000 fuels are light oils dominated by hydrocarbons with carbon numbers from 13 to 25. These oils do not form emulsions at sea which reduces their persistence. Compared to a fresh crude, they have fewer volatile components, leading to a lower initial loss through evaporation and dissolution. However, due to the low viscosity and thin films generally formed, these oils are relatively easily entrained into the water column given enough wind. These oils therefore rely mainly on ocean turbulence and biodegradation for dispersion and reduction of harmful concentrations in the marine environment. On the other hand, the IFO oil consists mainly of components with carbon numbers larger than 25 and will readily form an emulsion with seawater. Its biodegradability is low, which combined with increased viscosity from water uptake leads to more persistent presence on the ocean surface.

To illustrate the potential impact on pelagic organisms of the three fuel oils, we investigated a scenario of an accidental oil spill at the inlet of Isfjorden. The location of the oil spill was identical to one investigated previously for the Norwegian Coastal Administration. To highlight the different environmental footprints of the oils, we selected a time period of simulations where the direction of wind led to a worst-case scenario for the location in terms of concentration in the seawater. The worst case was considered to be the case where the oil is transported by wind into Grønfjorden, south-east of the discharge point. Within Grønfjorden, the constraints of the narrow fjord limit the extent of horizontal mixing, leading to less overall dilution compared to a spill at open sea.

Table 3.2. Input parameters for oil spill simulation in Isfjorden.

	Value	Unit
Release start time	2009-04-13 00:00	-
Release duration	3	Hours
Simulation duration	7	Days
Release quantity	2000	m^3
Latitude	78.164397	Degrees north positive
Longitude	13.771562	Degrees east positive
Simulation timestep	15	Minutes
Output timestep	1	Hour
Sea temperature	4	Degrees Celsius
Concentration grid horizontal resolution	100	m
Concentration grid vertical resolution	5	m

Ocean current data used for the simulation come from the SINMOD model run on a 4 km resolution. Since the 4 km input domain does not cover the entire simulation domain due to proximity to shore oil in these areas only experience horizontal transport from the wind through the windage factor set to 3.5 of the wind speed. The composition of the three oils as used in the OSCAR simulation is given in Table 3.3.

Table 3.3. Composition of DMA, MGO and IFO oils as used in OSCAR simulations. DMA and MGO have been characterized analytically while the IFO composition have been estimated from its boiling curve relative to that of the Statfjord oil since no analytical characterization was available.

	DMA	MGO	IFO
	MGO1000	**MGO500**	**IFO-LS**
C1-C4 gasses	0.000	0.000	0.000
C5-saturates	0.000	0.000	0.000
C6-saturates	0.094	0.245	0.000
Benzene	0.006	0.005	0.000
C7-saturates	0.300	0.250	0.000
C1-Benzene	0.067	0.065	0.000
C8-saturates	0.333	0.435	0.000
C2-Benzene	0.196	0.513	0.000
C9-saturates	0.210	0.357	0.000
C3-Benzene	0.344	1.130	0.164
C10-saturates	1.450	2.000	0.427
C4 and C4 Benzenes	0.068	0.115	0.015
C11-C12	3.332	9.685	1.075
Phenols	0.000	0.000	0.002
Naphthalenes 1	0.896	0.305	0.058
C13-C14	10.704	10.995	1.162
UCM: C10 to C36	0.000	0.000	0.093
Naphthalenes 2	1.903	0.478	2.197
C15-C16	8.397	11.622	1.802
PAH 1	1.057	0.453	0.078
C17-C18	13.443	21.847	3.373
C19-C20	18.200	30.700	2.591
C21-C25	29.643	7.117	7.752
PAH 2	1.857	0.583	0.123
C25+	7.500	1.100	79.088

4 Results and Discussion

4.1 Chemical characterization of LE-WAFs of fuel oils

The LE-WAFs of the three fuel oils differ in their chemical composition (Table **4.1**). The total WAF concentrations measured as the sum of volatile organic components (VOC, C5-C9) and total extractable material (TEM) differed markedly, MGO1000 being highest and double the concentrations in the MGO500 and IFO (Figure **4.1**A). The IFO had only miscible levels of VOC, and the VOC of the two diesels was dominated by BTEX, C3- and C4-benzenes (Figure **4.1**B). All had considerable concentrations of SVOC (Figure **4.1**C), dominated by naphthalenes, but also high concentrations of dibenzofuran, acenaphthene, C0-C1-phenanthrenes and fluorenes (Figure **4.1**). Low concentrations of the heavier 4-6 ring PAHs were found, reflecting their low water solubility. In general, the MGO1000 fuel oil displayed the highest concentrations of most identified/resolved and unresolved (UCM) components. This is in line with previous reports on solubility of fuel oil components (Faksness and Altin, 2017). Additional information regarding weathering properties of the fuel oils can be found in Hellstrøm (2017).

Table 4.1: Chemical composition of undiluted (100%) LE-WAFs sampled at the end of WAF generation. All concentrations are given as µg/L.

	MGO500	MGO1000	IFO-LS
Sum VOC	**454,7**	**243,0**	**1,4**
Sum BTEX	205,1	83,9	1,4
Sum C3-benzenes	148,1	103,4	0,0
Sum C4-benzenes	64,6	39,1	0,0
Sum C5-benzenes	12,9	9,0	0,0
Other VOC	24,0	7,6	0,0
Sum SVOC	**114,8**	**295,5**	**138,9**
Sum Decalins	0,39	0,16	0,06
Sum Naphthalenes	97,7	252,0	121,5
Sum 2-3-rings (excl. NAPHs)	14,1	40,1	11,4
Sum 4-6-rings	0,30	1,01	0,26
T-PAH	112,1	293,1	133,2
T-PAH (excl NAPHs)	14,4	41,1	11,7
Sum Phenols	2,3	2,2	5,6
Total WAF (Sum C_5-C_{36})	**996,2**	**1551,6**	**643,8**
TEM (Sum C_{10}-C_{36})	**541,5**	**1308,6**	**642,4**
UCM	**426,7**	**1013,1**	**503,5**

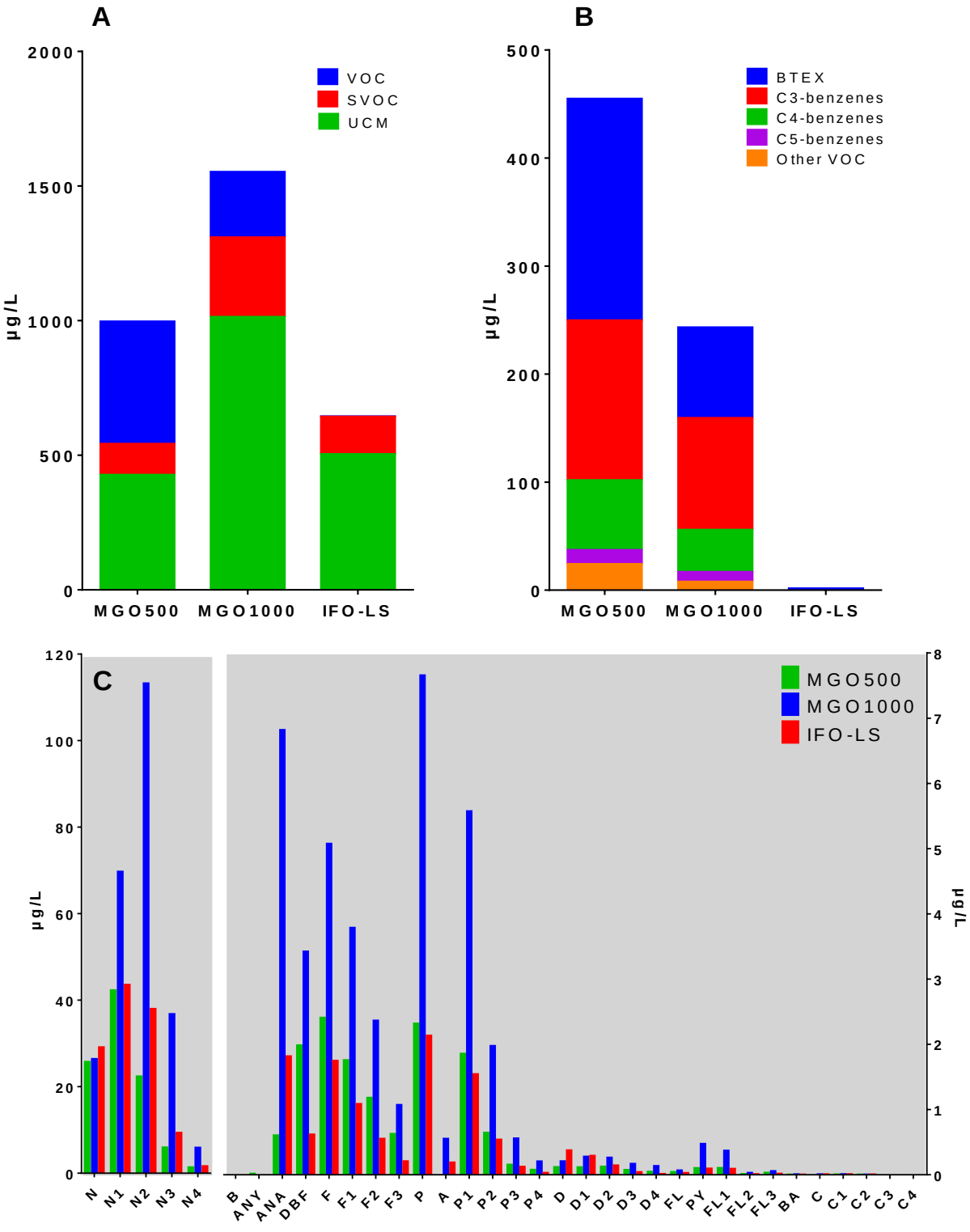

Figure 4.1: Chemical composition of WSFs (100%). A: Separated into VOC, SVOC and unresolved complex material (UCM). B: VOC composition only. C: Speciated composition of individual PAHs. Note different scaling on the axes. All concentrations are given in µg/L.

4.2 Chemical composition of exposure solutions

All prepared exposure solutions were analysed for TEM and SVOC using GC-FID and GC-MS, respectively, at onset of exposure and results are given in Table **4.2**. As expected, the concentration series for MGO1000 was at a higher level than for the other two fuel oils. There was also a significant loss of components during the first 48h exposure as evidenced by analyses of the T48 samples of the 100% solutions. The loss occurs due to evaporation, adhesion to glass walls and through bioconcentration in exposed eggs. Refilling with fresh exposure solutions was done at 48h exposure in order to limit this effect, and it is expected that the lowest levels embryos were exposed to occurred after 48 h as less would adhere to the glasses after refilling. Evaporation would be the same throughout the whole exposure period. Using static exposures in open containers is not optimal for generating effect levels. Optimally constant exposure concentrations should be used. In our experiments we made sure to assess loss by measuring the concentration in the highest exposure solution halfway into the experiments when exposure solutions were renewed. We have, however, related effects observed in fish to the TEM concentrations measured prior to exposure.

Table 4.2: Chemical composition of all diluted LE-WAFs sampled at onset of exposure of fish embryos and for the 100% WAF sampled after 48 h exposure (T48). All concentrations are given as µg/L.

		TEM (C_{10}-C_{36})	T-PAH (44 PAHs)	T-PAH (excl. NAPHs)	Sum 3-ring PAHs (FLU+PHE+DBT)
CTRL	**Sea water**	0,0	0,2	0,0	0,0
MGO500	**6%**	11,1	9,7	0,9	0,7
	12%	36,0	19,5	1,7	1,4
	25%	118,0	37,5	3,5	2,8
	50%	249,6	70,7	7,9	6,4
	100%	541,5	112,1	14,4	11,5
	100% T48	278,9	22,9	4,1	3,5
MGO1000	**6%**	56,3	45,5	2,6	1,9
	12%	110,3	84,4	5,2	3,8
	25%	278,9	122,3	10,2	7,4
	50%	611,9	198,9	21,4	15,4
	100%	1308,6	293,1	41,1	29,9
	100% T48	443,0	65,7	7,9	6,5
IFO-LS	**6%**	28,3	18,3	0,7	0,5
	12%	69,4	37,6	1,5	1,2
	25%	125,4	60,8	3,0	2,3
	50%	265,5	89,5	6,0	4,6
	100%	642,4	133,2	11,7	9,0
	100% T48	309,2	32,5	2,4	2,0

4.3 Hatching and survival

Hatching success was relatively high for all treatments (>80%), and there was no clear relationship with concentration. Significantly lower hatching success were only observed in a few groups (MGO500: 12% ($p<0.01$), 25% ($p<0.05$), 100% ($p<0.05$). IFO-LS: 100% ($p<0.001$)). Hatching was, however, induced significantly earlier than controls for embryos exposed to all fuel oils and concentrations ($p<0.0001$), but also here there is no clear concentration-dependent pattern. For the lowest exposure concentrations, larvae hatched 4 days earlier than in controls. This in contrary to previous experiments with cod exposed to WAFs

of crude oils, where a delay in hatching was observed (Hansen et al., 2018a). Reduced larvae survival was observed for all fuel oil exposures, being significantly lower for MGO500 (6% ($p<0.001$), 25% ($p<0.01$), 50% ($p<0.0001$)), MGO1000 (6%, 25% and 50% ($p<0.0001$)) and IFO-LS (6% ($p<0.001$), 12% ($p<0.01$), 50% ($p<0.0001$)). The relationship between larvae survival and exposure concentrations were ∩-shaped. This does not appear to be an experimental artefact as it was evident for LE-WAFs from all three fuel oils. The length of time larvae were monitored was also different between the groups due to differences in hatching time, e.g. for the lowest exposure concentrations, where larvae hatched 4 days earlier than controls, the cumulative larvae mortality was higher than controls, but they were also monitored as larvae for 4 additional days. The measurements of survival may also well be affected by the larvae behaviour as, particularly for the high concentrations, the larvae were not moving very much, and we had to test for survival using the microscope to see heart beats. This was, however, done consistently only for the highest exposure concentrations.

4.4 Larvae condition

At 3 dph, larvae for every treatment were photographed, and images were used to assess morphometry, development and deformations. Three standard measures of development; body area, standard length and myotome height, all displayed clear concentration-dependent reductions (Figure 4.2A-C). Compared to control performance, body area and myotome height was smaller only for larvae exposed to 100% MGO ($p<0.0001$). For larvae standard length, exposed larvae were significantly shorter compared to control for all exposure concentrations of MGO500, MGO1000 (except 12%) and IFO-LS.

The yolk fraction (fraction of the body area containing the yolk sac) was significantly higher compared to controls for all treatments except 6% MGO500-exposure. This effect was also observed in a concentration-dependent manner for all fuel oils (Figure 4.2D). The higher yolk fraction is a result of reduced consumption of the yolk sac in exposed larvae resulting in smaller-sized larvae. The underlying mechanism behind this effect is unclear.

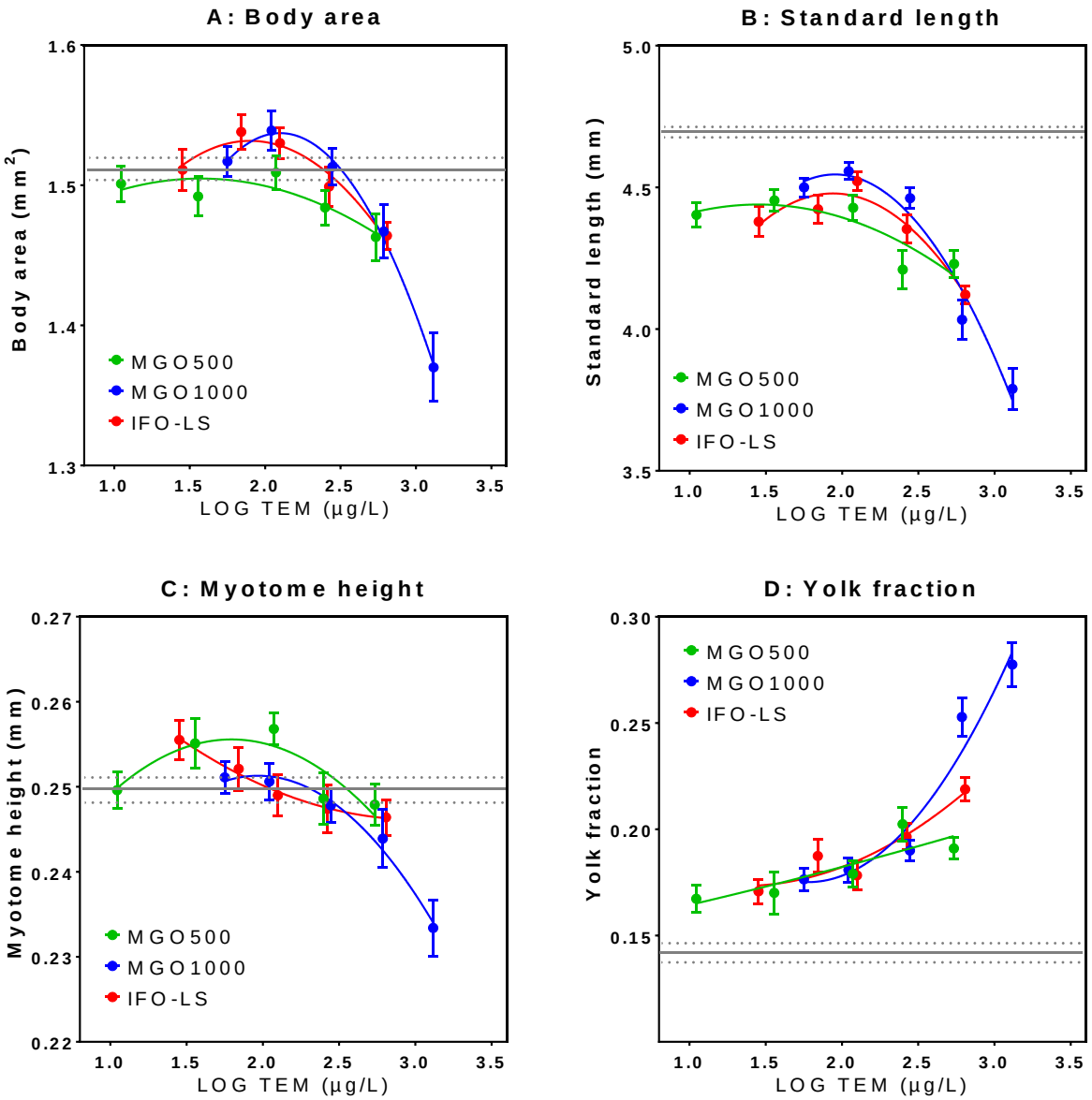

Figure 4.2: Developmental data of cod larvae exposed MGO500 (green), MGO1000 (blue) and IFO (red) as a function of exposure concentration (µg/L TEM). Data given as average ± SEM (N=28-32). Control values are given as grey line (broken line: SEM, N=45).

4.5 Larvae deformations

It has been well documented that embryonic exposure to oil components from crude oil and produced water cause deformed larvae of cold-water marine fish (Hansen et al., 2018a; Hansen et al., 2019; Sørhus et al., 2015; Sørhus et al., 2016). Morphological measurements of larvae from our experiments shows that the same occurs following exposure to dissolved components of fuel oils (Figure 4.3).

Measurements of deformations in the cranium and jaw regions show that larval eye diameter and deformation severities are affected in a concentration-dependent manner. Significantly smaller eyes and shorter distances between eyes and forehead were observed in larvae after being exposed to the 50 and

100% WAFs of MGO500, MGO1000 and IFO-LS ($p<0.01$) (Figure 4.3A and B). Ranking of craniofacial and jaw deformations based on a system adopted from Sørhus et al (2015) where larvae were assigned numbers 1-3 based on deformation appearance (1=normal, 2=some deformations and 3=severe deformations) also displayed clear concentration-dependent responses (Figure 4.3C and D). Statistical analyses showed that significantly higher deformation severities were found in MGO500 (6%: $p<0.05$, 50%: $p<0.001$ and 100%: $p<0.0001$), MGO1000 (50 and 100%: $p<0.0001$) and IFO-LS (50%: $p<0.05$, 100%: $p<0.0001$).

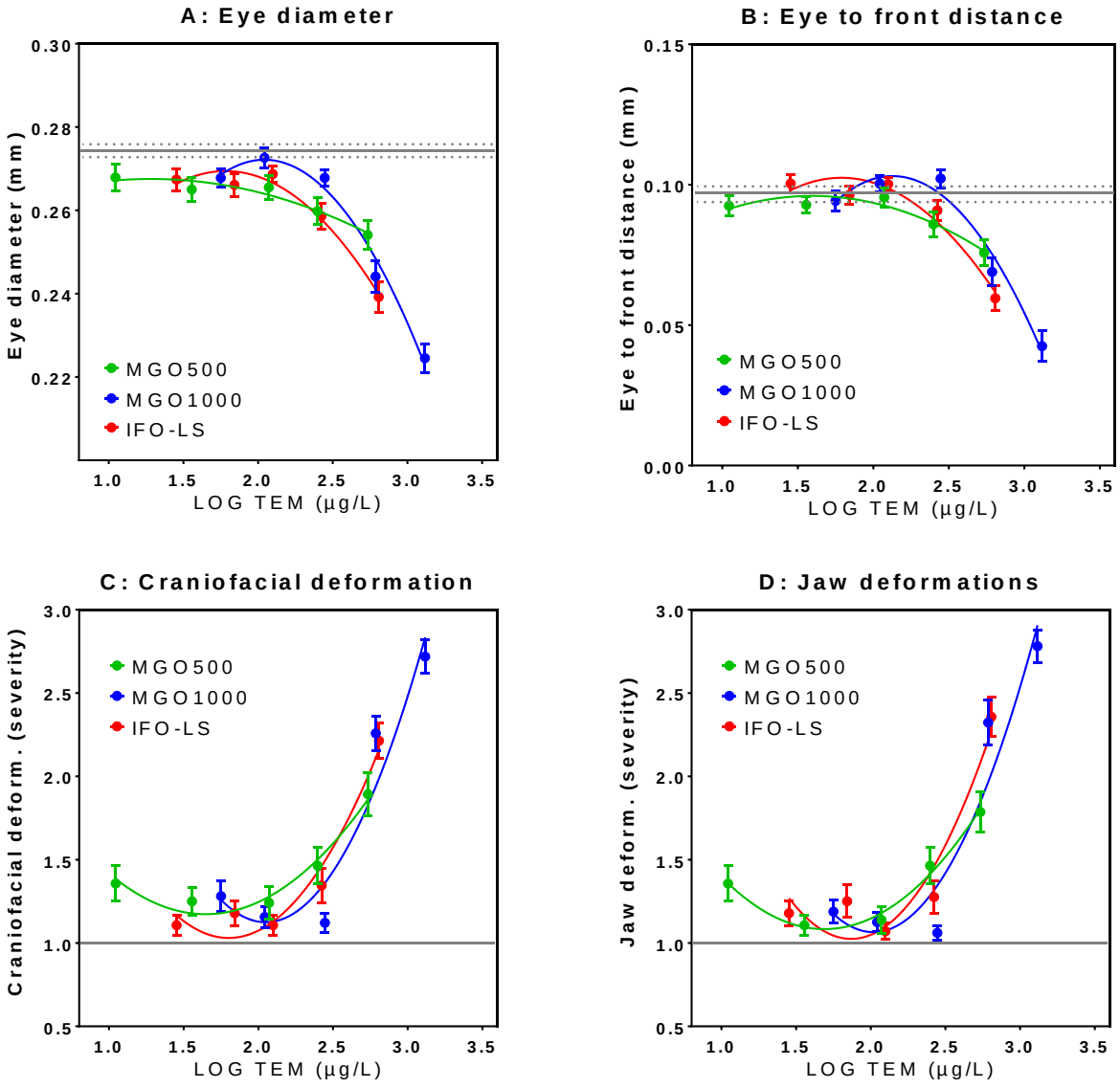

Figure 4.3: Deformation data of cod larvae exposed to MGO500 (green), MGO1000 (blue) and IFO (red) as a function of exposure concentration (µg/L TEM). A: Eye diameter. B: Distance between eye and forehead. C: Craniofacial deformation severity. D: Jaw deformation severity. Data given as average ± SEM (N=28-32). Control values are given as grey line (broken line: SEM, N=45).

4.6 Cardiac toxicity

It has been hypothesised that severe oil-induced larvae deformations is a result of the impacts of oil components (mainly three-ringed PAHs) on cardiac development and function (Incardona et al., 2009; Incardona et al., 2004), and cardiotoxicity has previously been shown in cold-water marine fish, like cod and haddock (Hansen et al., 2018a; Hansen et al., 2019; Sørhus et al., 2015; Sørhus et al., 2016). We observed reduced larvae heart rate in a concentration-dependent manner for MGO1000 and IFO-LS (Figure 4.4A) being significantly lower for MGO1000 50% ($p<0.05$), MGO1000 100% ($p<0.001$) and IFO-LS 100% ($p<0.01$). A typical cardiotoxic feature is a non-functional ventricle, a so-called 'silent ventricle' which also was apparent (Figure 4.4B) and significant in hatched larvae from the MGO500 100% ($p<0.0001$), MGO1000 50% ($p<0.0001$) and 100% ($p<0.0001$), and IFO-LS 50% ($p<0.01$) and 100% ($p<0.0001$). Pericardial edema severity was also assessed in all sampled larvae (Figure 4.4C), and significantly higher severities were observed in 100% MGO500 ($p<0.0001$), 50% and 100% MGO1000 ($p<0.0001$) and 100% IFO ($p<0.0001$).

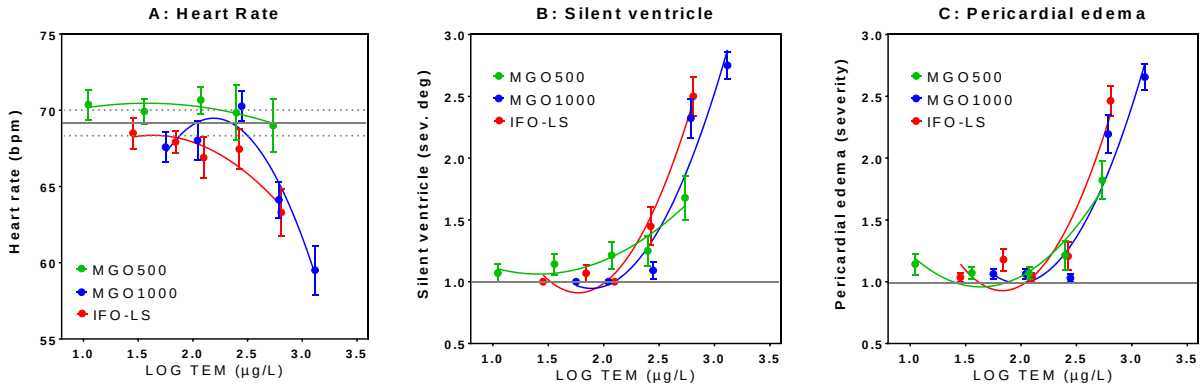

Figure 4.4: Cardiotoxicity data of cod larvae exposed to MGO500 (green), MGO1000 (blue) and IFO (red) as a function of exposure concentration (µg/L TEM). A: Heart rate. B: Silent ventricle severity. C: Pericardial edema severity. Data given as average ± SEM (N=28-32). Control values are given as grey line (broken line: SEM, N=45). No indications of silent ventricle (B) or pericardial edema (C) were observed in controls.

4.7 Threshold levels for toxicity

The aim of the project was to determine no-effect concentrations (NECs) for WSFs of the different fuel oils for estimating 'safe' water concentrations. Based on previous experiments using marine algae and copepods, diluting the WSFs to 6% was sufficient to not causing any toxic effect. However, when using a 4-day toxicity test with highly sensitive cod embryos, it was not possible to determine NECs for many of the endpoints assessed. Although concentration-dependent responses were observed for most of the endpoints, some displayed significant differences compared to controls also for the lowest exposure concentrations (6% WSF). Thus, NECs are not easily verified. In Table 4.3, a summary of the statistical analyses using One-way ANOVA with Dunnett's multiple comparison post hoc test to compare treated groups to controls are presented. The table also includes concentrations of different OSCAR groups in exposure solutions.

Table 4.3: Summary table of concentrations of OSCAR component groups in different treatments and statistics comparing different treatments to controls using One-way ANOVA with Dunnett's multiple comparisons test. Responses in treatments were significantly different from control when asterisks are shown: *p<0.05, **p<0.01, **p<0.001, ***p<0.0001 and p<0.00001. ns=not significantly different from controls (p>0.05).

	MGO500					MGO1000					IFO-LS				
% LE-WAF	6%	12%	25%	50%	100%	6%	12%	25%	50%	100%	6%	12%	25%	50%	100%
TEM	*11.1*	*36.0*	*118.0*	*249.6*	*541.5*	*56.3*	*110.3*	*278.9*	*611.9*	*1309*	*28.3*	*69.4*	*125.4*	*265.5*	*642.4*
Napht+PAH	*9.7*	*19.5*	*37.5*	*70.7*	*112.1*	*45.5*	*84.4*	*122.3*	*198.9*	*293.1*	*18.3*	*37.6*	*60.8*	*89.5*	*133.2*
Napht-1 + -2	*8.8*	*17.6*	*33.7*	*62.1*	*96.3*	*42.4*	*78.4*	*110.7*	*174.6*	*246.1*	*17.5*	*35.9*	*57.4*	*82.7*	*119.9*
PAH-1 + -2	*0.9*	*1.9*	*3.8*	*8.6*	*15.7*	*3.0*	*5.9*	*11.7*	*24.3*	*47.0*	*0.8*	*1.7*	*3.4*	*6.8*	*13.3*
Hatching success	ns	**	*	ns	*	ns	ns	ns	ns	ns	ns	ns	ns	ns	***
Hatch timing	****	****	****	****	****	****	****	****	****	****	****	****	****	****	****
Larvae survival	***	ns	**	****	ns	****	ns	****	****	ns	***	**	ns	****	ns
Yolk area	ns	ns	**	****	****	**	****	****	****	****	*	****	***	****	****
Body area	ns	ns	ns	ns	ns	ns	ns	ns	ns	****	ns	ns	ns	ns	ns
Length	****	**	***	****	****	*	ns	***	****	****	****	***	*	****	****
Yolk fraction	ns	*	***	****	****	**	***	****	****	****	*	****	***	****	****
Eye diameter	ns	ns	ns	**	****	ns	ns	ns	****	****	ns	ns	ns	***	****
Myotome height	ns	ns	ns	ns	ns	ns	ns	ns	ns	****	ns	ns	ns	ns	ns
Eye to front dist.	ns	ns	ns	ns	***	ns	ns	ns	****	****	ns	ns	ns	ns	****
Heart rate	ns	ns	ns	ns	ns	ns	ns	ns	*	****	ns	ns	ns	ns	**
Silent ventricle	ns	ns	ns	ns	****	ns	ns	ns	****	****	ns	ns	ns	**	****
Craniofacial deform.	*	ns	ns	***	****	ns	ns	ns	****	****	ns	ns	ns	*	****
Jaw deform.	*	ns	ns	***	****	ns	ns	ns	****	****	ns	ns	ns	ns	****
Pericardial edema	ns	ns	ns	ns	****	ns	ns	ns	****	****	ns	ns	ns	ns	****

To determine threshold levels, there is a need to normalize the toxicity data to the exposure concentration of the relevant toxicity-driving components. The main driver for acute toxicity (mortality) is expected to be the naphthalenes, based on their high solubility. For developmental effects, which is a different mode of toxic action than acute toxicity, PAHs are generally considered the most important contributors, but this has been debated for decades (Barron et al., 1999). Ongoing (Research Council-funded) research in the PW-Exposed- and EGGTOX-projects, led by SINTEF Ocean and Institute of Marine Research, respectively, aims at increasing the understanding of oil toxicity to fish ELS and identify the main toxicity drivers. As the current understanding of which components cause developmental toxicity to fish ELS is limited, most studies use total PAH (T-PAH) for providing thresholds for toxicity. Although this is practical, it is, however, probably not correct as single PAH studies provide magnitude higher thresholds for toxicity than mixtures of petrogenic components (e.g. WAFs). Furthermore, it has been shown that during biodegradation, dissolved oil components are equally toxic after 3-weeks degradation when only miscible levels of PAHs are remaining (Hansen et al., 2018a). For the oil spill scenarios, we tested using all components (total hydrocarbon), all T-PAH and T-PAH excluding naphthalenes.

4.8 OSCAR simulations of Arctic fuel oil spills

Identical oil spill scenarios (Table 4.3) were run for each of the three fuel oils MGO500, MGO1000, and IFO-LS. The initial trajectory of the oils were toward the south east into Grønfjorden where the oil remained for the duration of the simulations (Figure 4.5). This represents a worst-case scenario in which dissolved oil is limited in terms of dilution, resulting in water concentrations higher than they would have been if the oil drifted east or west.

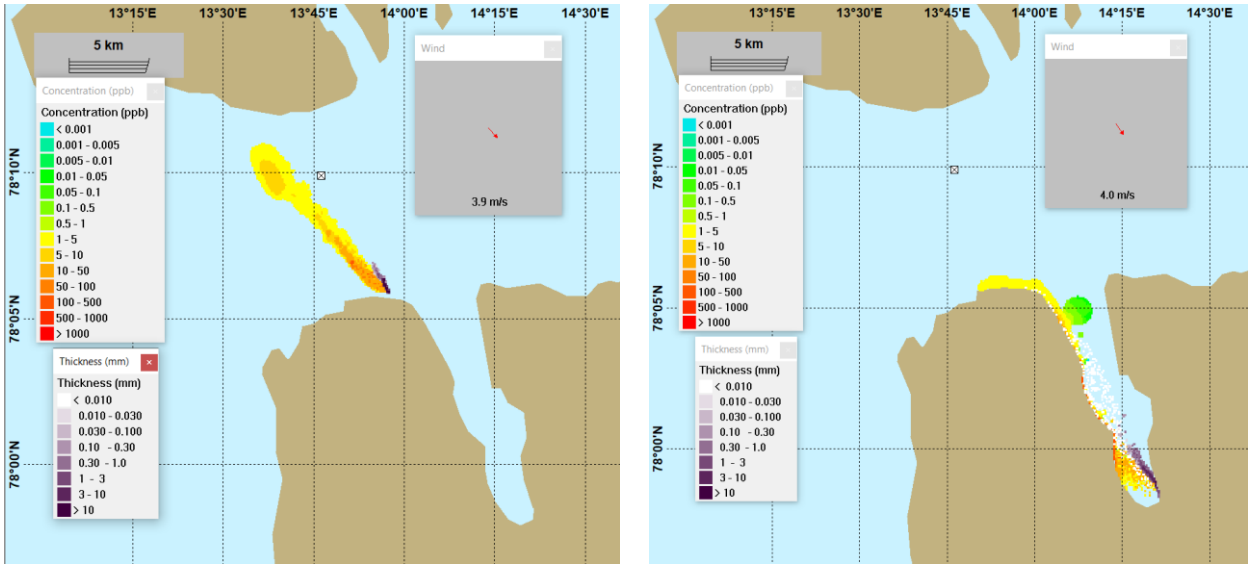

Figure 4.5. Initial oil trajectory for oil spill simulations at 14 hrs (left) and 45 hrs (right) after simulation start. Surface oil is transported due the wind into Grønfjorden where it remained for the remainder of the simulation. The legends show colour for concentration of dissolved oil (ppb) and thickness of surface oil (mm). The white cross indicates the release point.

To assess the potential exposure to fish eggs in the water column, we calculated timeseries of volumes of seawater with concentrations of oil above thresholds found in the toxicological assay (Table 4.3). As mentioned previously, we were unable to establish 'No effect concentrations' based on the toxicity tests because we observed significant toxicity at the lowest concentrations used in our experiments. We did, however, run simulations where we estimated water volumes with a TEM concentration higher than 11.1 µg/L, which was the lowest TEM concentration measured in the WAFs (Table **4.2**). In the modelling, total concentrations are denoted total hydrocarbon content (THC). Due to the higher content of dissolvable components, the MGO1000 fuel oil displayed up to a factor of four higher THC concentrations than the other two fuel oils during the scenario time window, peaking approximately 1 day after release. The water volumes containing >11.1 µg/L THC were similar between the MGO500 and IFO-LS throughout the simulation.

Due to the expectations that PAHs are driving sublethal effects in fish early life stages, we also performed simulations estimating water concentrations for sum of all PAHs (Figure 4.6B) and sum of PAHs without naphthalenes (Figure 4.6C). This was done because naphthalenes are not considered a major driver for developmental effects, but primarily related to acute toxicity (mortality). Here, we used a threshold value of 0.1 µg/L and estimated time-series of water volumes with concentrations >0.1 µg/L. This threshold was chosen based on previous OSCAR simulations performed in the SYMBIOSES project (Carroll et al., 2018). Carroll et al (2018) used threshold levels for immediate mortality of 1.0 µg/L T-PAH and 0.1 µg/L T-PAH for delayed developmental effects. Also when assessing water volumes with T-PAH thresholds, the MGO1000 stands out having a significantly higher influence area than the two other fuel oils in the simulations (Figure 4.6B). The naphthalenes were the most important contributors to the PAH composition in the water because when we estimated water volumes with PAH concentrations >0.1 µg/L, the volumes were much lower (Figure 4.6). Here the two MGO fuel oils displayed similar temporal trends and higher than the IFO-LS.

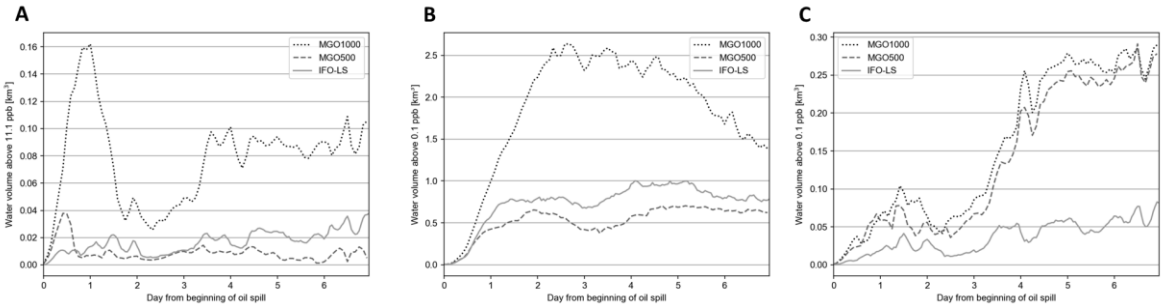

Figure 4.6. Timeseries of volumes of contaminated water with concentrations above toxicity thresholds. A: THC above 11.1 µg/L. B: Total PAH (Sum NAPH 1, NAPH 2, PAH 1 and PAH 2) above 0.1 µg/L. C: Total PAH excluding naphthalenes (Sum PAH1 and PAH2) above 0.1 µg/L.

5 Conclusions and Gaps of Knowledge

The main conclusions from this work may be summed up in the following:

- The chemical composition of the three oils tested were different, and the composition of MGO1000 facilitated dissolution as higher concentrations of PAHs were found in the WAF for this oil.
- WAF of all three fuel oils displayed embryo- and larvae toxicity, and this was observed even after exposure to the most diluted WAF (6%) used in the exposure experiments.
- Severe larvae deformations were only observed after exposure to less diluted WAFs (50-100%).
- Based on concentration (using TEM), the three oils displayed comparable toxicity, but the highest toxicity levels were observed for highest MGO1000 treatment (which also displayed the highest concentration).
- Simulating fuel oil spills in Isfjorden using OSCAR showed that the MGO1000 displayed the highest water volumes expected to cause fish ELS toxicity (threshold set at 11.1 µg TEM/L).
- Using NEC from the literature (0.1 µg/L) as threshold for toxicity in the OSCAR simulation, also suggested that MGO1000 displayed the highest water volume above threshold, but the MGO500 and MGO1000 was similar when only PAHs were included in the simulation.

The main gaps of knowledge are related to four main topics; knowledge about more fuel oils, identification of embryotoxicity drivers, toxicokinetics and population dynamics:

Knowledge about more fuel oils. We tested three different fuel oils in the present project, however, the range of different fuel products on the market is large and expanding. A range of fuel oils has been tested for toxicity on phytoplankton and zooplankton in previous SINTEF-projects, but this report represents the only tests where fish early life stages have been included in the toxicity assessment. Preferably all fuel products should be tested on three levels of the food chain, and particularly it is of importance to test the most sensitive species and life stages.

Identification of toxicity drivers. In order to perform better risk and damage assessment of fuel oil spills it is important to identify the oil components causing toxicity. In the current report and in most of the literature, TEM or T-PAH has been used as a proxy for estimating toxicity thresholds. Literature has shown that relating toxicity to PAH concentrations underestimates toxicity in fish ELS tests (Barron et al., 1999; Barron and Holder, 2003), and that other unresolved components are likely contributors to toxicity (Melbye et al., 2009; Sørensen et al., 2019).

Toxicokinetics parameter estimations. In the present work, the influence areas were determined based simulations using water concentration thresholds determined by the experiments (and from the literature). However, exposures change dynamically in the field resulting in fluctuating exposure concentrations as a function of time. For fish eggs to be affected by fuel oil components, toxic components need to be taken up from the water into the body. Thus, determination of exposure doses (body burdens) causing toxic effects is more relevant for determining the toxic potential of a spill than using water concentrations. This is possible using the OSCAR model, however, it will need relevant toxicokinetics model parameter, particularly bioconcentration factors and elimination rates, relevant for the toxicity-driving oil components and organisms at risk. This enables a more realistic modelling approach to estimate impacts of fuel oil spills as it will account for fluctuations in exposure concentrations as a function of time and focus on toxicity based on accumulated in fish eggs.

Population dynamics. In the present work, Atlantic cod was used as a model species due to its relevance for cold marine environment and its known sensitivity to oil exposure. Atlantic cod does not spawn and reproduce in the area where the oil spill simulations were located. Relevance of the modelling scenarios will greatly improve by local knowledge regarding spatial and temporal distribution of relevant fish eggs and larvae. In addition, research has suggested that some Arctic species, like the polar cod (*Boregadus saida*) is particularly sensitive to oil exposure (Nahrgang et al., 2016).

6 References

Aurand, D., Coelho, G.M., 1996. Proceedings of the Fourth Meeting of the Chemical Response to Oil Spills: Ecological Effects Research Forum., in: Ecosystem Management & Associates, P., VA. (Ed.), p. 50.

Barron, M., Podrabsky, T., Ogle, S., Ricker, R., 1999. Are aromatic hydrocarbons the primary determinant of petroleum toxicity to aquatic organisms? Aquatic Toxicology 46, 253-268.

Barron, M.G., Holder, E., 2003. Are exposure and ecological risks of PAHs underestimated at petroleum contaminated sites? Human and Ecological Risk Assessment 9, 1533-1545.

Carroll, J., Vikebø, F., Howell, D., Broch, O.J., Nepstad, R., Augustine, S., Skeie, G.M., Bast, R., Juselius, J., 2018. Assessing impacts of simulated oil spills on the Northeast Arctic cod fishery. Marine Pollution Bulletin 126, 63-73.

Faksness, L.G., Altin, D., 2017. WAF and toxicity testing of diesel and hybrid oils. SINTEF Ocean, Trondheim, pp. 1-38.

Hansen, B.H., Farkas, J., Nordtug, T., Altin, D., Brakstad, O.G., 2018a. Does Microbial Biodegradation of Water-Soluble Components of Oil Reduce the Toxicity to Early Life Stages of Fish? Environmental Science & Technology 52, 4358-4366.

Hansen, B.H., Sorensen, L., Carvalho, P.A., Meier, S., Booth, A.M., Altin, D., Farkas, J., Nordtug, T., 2018b. Adhesion of mechanically and chemically dispersed crude oil droplets to eggs of Atlantic cod (Gadus morhua) and haddock (Melanogrammus aeglefinus). The Science of the total environment 640-641, 138-143.

Hansen, B.H., Sørensen, L., Størseth, T.R., Nepstad, R., Altin, D., Krause, D., Meier, S., Nordtug, T., 2019. Embryonic exposure to produced water can cause cardiac toxicity and deformations in Atlantic cod (Gadus morhua) and haddock (Melanogrammus aeglefinus) larvae. Marine Environmental Research 148, 81-86.

Hellstrøm, K., 2017. Weathering Properties and Toxicity of Marine Fuel Oils - Summary report, in: SINTEF (Ed.), pp. 1-82.

Incardona, J.P., Carls, M.G., Day, H.L., Sloan, C.A., Bolton, J.L., Collier, T.K., Scholz, N.L., 2009. Cardiac Arrhythmia Is the Primary Response of Embryonic Pacific Herring (Clupea pallasi) Exposed to Crude Oil during Weathering. Environmental Science & Technology 43, 201-207.

Incardona, J.P., Collier, T.K., Scholz, N.L., 2004. Defects in cardiac function precede morphological abnormalities in fish embryos exposed to polycyclic aromatic hydrocarbons. Toxicology and Applied Pharmacology 196, 191-205.

Kystverket, 2014. Beredskapsanalyse for skipstrafikken i områdene rundt Svalbard og Jan Mayen, in: Kystverket (Ed.), pp. 1-159.

Melbye, A.G., Brakstad, O.G., Hokstad, J.N., Gregersen, I.K., Hansen, B.H., Booth, A.M., Rowland, S.J., Tollefsen, K.E., 2009. Chemical and toxicological characterization of an unresolved complex mixture-rich biodegraded crude oil. Environmental Toxicology and Chemistry 28, 1815-1824.

Nahrgang, J., Dubourg, P., Frantzen, M., Storch, D., Dahlke, F., Meador, J.P., 2016. Early life stages of an arctic keystone species (Boreogadus saida) show high sensitivity to a water-soluble fraction of crude oil. Environmental Pollution 218, 605-614.

Nepstad, R., Davies, E., Altin, D., Nordtug, T., Hansen, B.H., 2017. Automatic determination of heart rates from microscopy videos of early life stages of fish. Journal of Toxicology and Environmental Health, Part A 80, 932-940.

Singer, M.M., Aurand, D., Bragin, G.E., Clark, J.R., Coelho, G.M., Sowby, M.L., Tjeerdema, R.S., 2000. Standardization of the preparation and quantitation of water-accommodated fractions of petroleum for toxicity testing. Marine Pollution Bulletin 40, 1007-1016.

Sørensen, L., Hansen, B.H., Farkas, J., Donald, C.E., Robson, W.J., Tonkin, A., Meier, S., Rowland, S.J., 2019. Accumulation and toxicity of monoaromatic petroleum hydrocarbons in early life stages of cod and haddock. Environmental Pollution 251, 212-220.

Sørhus, E., Edvardsen, R.B., Karlsen, Ø., Nordtug, T., Van Der Meeren, T., Thorsen, A., Harman, C., Jentoft, S., Meier, S., 2015. Unexpected interaction with dispersed crude oil droplets drives severe toxicity in atlantic haddock embryos. Plos One 10.

Sørhus, E., Incardona, J.P., Karlsen, Ø., Linbo, T., Sørensen, L., Nordtug, T., van der Meeren, T., Thorsen, A., Thorbjørnsen, M., Jentoft, S., Edvardsen, R.B., Meier, S., 2016. Crude oil exposures reveal roles for intracellular calcium cycling in haddock craniofacial and cardiac development. Scientific Reports 6, 31058.

US-EPA, 2006. Method 8260C, 2006. Volatile organic compounds by gas chromatography/mass spectrometry (GC/MS).

US-EPA, 2013. EPA Method 8015D (SW-846): Nonhalogenated Organics Using GC/FID. US-EPA.

USEPA, 1996. Method 3510C: Separatory funnel liquid–liquid extraction.

USEPA, 2007. Method 8270D: Semivolatile Organic Compounds by GC/MS.